Available online at www.sciencedirect.com
SCIENCE DIRECT®
Computers, Environment and Urban Systems
29 (2005) 718–734
Computers, Environment and Urban Systems
www.elsevier.com/locate/compenvurbsys

Evaluation of algorithms developed for adaptive grid air quality modeling using surface elevation data

Maudood N. Khan [a,*], Mehmet T. Odman [a], Hassan A. Karimi [b]

[a] *School of Civil and Environmental Engineering, Georgia Institute of Technology, Atlanta, GA 30332-0512, USA*
[b] *Department of Information Science and Telecommunication, University of Pittsburgh, Pittsburgh, PA 15260, USA*

Received 1 September 2002; accepted 23 August 2004

Abstract

An adaptive grid model is being developed to reduce the resolution-related uncertainty in air quality predictions. By clustering the grid nodes in regions where errors in pollutant concentrations would potentially be large, the model is expected to generate much more accurate results than its fixed, uniform grid counterparts. The repositioning of grid nodes is performed automatically using a weight function that assumes large values when the curvature (change of slope) of the pollutant fields is large. Despite the movement of the nodes, the structure of the grid does not change: each node retains its connectivity to the same neighboring nodes. Since there is no a priori knowledge of the grid movement, the input data must be re-gridded after each adaptation step, throughout the simulation. Emissions are one of the major inputs and mapping them to the adapted grid is a computationally intensive task. Efficient intersection algorithms are being developed that take advantage of the unchanging grid structure.

Here, the grid node repositioning and intersection algorithms are evaluated using surface elevation data. Two elevation data sets are reduced to one-fourth of their sizes using uniform

* Corresponding author. Tel.: +1 404 363 7101.
E-mail address: maudood_khan@dnr.state.ga.us (M.N. Khan).

0198-9715/$ - see front matter
doi:10.1016/j.compenvurbsys.2004.08.002

as well as adaptive grids. The first data set contains important terrain features near the boundaries while the second has all of its features far away from the boundaries. The compression of the first data set using grid node repositioning results in a maximum error that is 25% smaller compared to a uniform grid with the same number of nodes. The maximum error associated with the adaptive grid compression of the second data set is 60% smaller compared to the uniform grid compression. These results show that the adaptive grid algorithm has the potential of significantly improving the accuracy of air quality predictions, especially when the regions of changing slope are far away from the boundaries. Indeed, in a preliminary air quality application, the adaptive grid displayed superior performance in capturing the details of plumes from a large number of emission sources. The algorithms are computationally efficient and the overhead involved in repositioning the grid nodes and intersecting the grid cells with emission sources is not limiting in air quality simulations.

Keywords: Air pollution model; Adaptive meshes; Emission processing; Grid adaptation; Geographic information system

1. Introduction

Emission control strategies that are being developed to improve air quality rely heavily on simulations with air quality models (AQMs). Control strategies can be very costly to implement and they have a direct bearing on public health and lifestyle. If the accuracy of AQM simulations can be improved, more effective strategies can be designed. One source of uncertainty in AQM simulations is attributed to the spatial resolution of the numerical grid, which is limited by the availability of computational resources. A large grid size is unable to resolve input data or capture the non-linear physical and chemical processes that occur over smaller spatial scales. To address this issue, nested grid or multiscale modeling techniques have been developed that use finer grid resolution in regions of interest and coarser grids elsewhere (Odman et al., 1997). Several AQMs have ''one-way'' nesting capability where the coarse grid simulation is used to set boundary conditions for the fine grid but the fine grid simulation has no feedback onto the coarse grid. A multiscale AQM that allows ''two-way'' interactions between various scales was developed by Kumar, Odman, and Russell (1994) and Boylan et al. (2002) based on the finite element transport scheme of Odman and Russell (1991a, 1991b). All these techniques are limited by not knowing, a priori, where to place the finer resolution grids, loss in solution accuracy due to grid interface problems (Alapaty, Mathur, & Odman, 1998), and the inability to adjust to dynamic changes in the solution. An alternative approach to achieving local resolution involves using dynamic adaptive grids, which are not subject to the aforementioned limitations. Adaptive grids have been applied to various problems in atmospheric modeling. Dietachmayer and Droegemeier (1992) used a variational formulation to adapt the grid and minimize the error in meteorological modeling. Skamarock and Kemp (1993) used a hierarchical grid approach to model compressible formulation of the atmospheric flow equations. Almgren, Bell, Collela,

Howell, and Welcome (1997) used a nested hierarchy of grids, with simultaneous refinement of grids in both space and time to resolve the release of hot gasses into the atmosphere. Tomlin, Berzins, Ware, Smith, and Pilling (1997) applied a three-dimensional adaptive grid technique to study atmospheric dispersion problems using a finite volume cell-vertex approach on unstructured grids (tetrahedral elements). Kessler (1999) used a dynamic adaptive grid to solve two-dimensional transport problems. More recently, Srivastava, McRae, and Odman (2000, 2001a, 2001b) designed an adaptive grid algorithm for use in air quality modeling. In this algorithm, using a weight function that represents the error in the solution (i.e., in pollutant fields), grid nodes are clustered in regions where they are needed the most.

Probably the most restrictive issue in the development of adaptive grid AQMs is the processing of emissions for a continuously moving grid. Emission inventories include hundreds of compounds emitted from a variety of sources ranging from large utility plants to motor vehicle tailpipes. Geographical information systems (GIS) are used to retrieve the raw emissions data from the inventories and generate gridded, time-varying emissions in terms of the chemical species represented in the models. In adaptive grid models, the shape and location of grid cells change after each adaptation. A source that lies in a grid cell might lie in another cell after adaptation. Therefore, the processing of emissions data must be performed in real time, after each adaptation of the grid. The task of locating a point (e.g., stacks), line (e.g., roads) or an area (e.g., farm) source within a grid is referred to as the *intersection* problem (Karimi, Brandymeyer, Wong, & Bourgeois, 1999). Efficient intersection algorithms are needed to reduce the overhead of re-gridding emission inputs in real time.

This paper describes the grid-node repositioning and emission source intersection algorithms, and discusses their performance in a test problem consisting of adapting a grid to surface elevation data. The reason for using elevation data in this exercise is the similarities between complex terrain and pollutant fields, in terms of changing slopes. The major difference between an elevation field and a pollutant field is that the former is static while the latter changes in time. However, in AQM simulations, the evolution of pollutant fields is captured in discrete time steps. Each time step is followed by a grid adaptation step such that the pollutant field can be better resolved. Hence, the test with surface elevation data emulates a single adaptation step of an actual AQM simulation where time evolution is stopped and the grid is adapted to the pollutant field. As long as the terrain is complex enough to imitate typical pollutant fields, this test may be viewed as a robust evaluation case for the grid-node repositioning algorithm. The test case also evaluates the point-source intersection algorithm in an indirect way. While the elevation of repositioned nodes is calculated, there is a need to locate the cell of the elevation data grid that contains the node location. While there are more efficient ways of performing this task, we use the point-source intersection algorithm, which was designed for a similar purpose: to locate the fixed position of a point source over a moving grid. This way we are able to evaluate both the grid-node repositioning and point source intersection algorithms in the same test.

2. Methodology

The adaptive grid methodology used here is based on the Dynamic Solution Adaptive Grid Algorithm (Benson & McRae, 1991). Since it is described in detail in Srivastava et al. (2000), it will only be highlighted here. The method employs a constant number of grid nodes that partition a rectangular domain into N by M quadrilateral grid cells. The nodes move throughout the simulation but the grid structure remains the same (i.e., topology does not change). In other words, each node is still connected to the same neighboring nodes but the length of the links and the area of the grid cells change. One of the advantages of using a structured grid is that, through a coordinate transformation, the non-uniform grid in the physical space can be mapped onto a uniform grid in the computational space. The solution of partial differential equations that govern atmospheric diffusion is simpler on a uniform grid. Another advantage is compatibility with the majority of existing AQMs. It is easier to follow new developments in atmospheric modeling with structured grids (and finite difference/volume methods) since they are much more common than unstructured grids (and the finite element method).

The movement of the nodes is controlled by a weight function whose value is proportional to the error in the solution. The nodes are clustered around regions where the weight function bears large values, thereby increasing the resolution where the error is large. Since the number of nodes is fixed, refinement of grid scales in regions of interest is accompanied by coarsening in other regions where the weight function has smaller values. This yields a continuous multiscale grid where the scales change gradually. Unlike nested grids, there are no grid interfaces, which may introduce numerous difficulties due to the discontinuity of grid scales. The availability of computational resources determines the number of grid nodes that can be afforded in any AQM. By clustering grid nodes automatically in regions of interest, computational resources are used in an optimal fashion throughout the simulation.

2.1. Weight function and grid node repositioning

The grid nodes are moved using a weight function along with a center-of-mass repositioning scheme. The weight function must be such that its value is large in regions where grid nodes need to be clustered. There are also some requirements for the resulting grid in order to assure an accurate numerical solution of governing partial differential equations. The grid must be free of highly skewed cells, and there must be a smooth transition from small to large cells with no voids in regions where the pollutant field is relatively uniform. Laflin and McRae (1996) developed a weight function that satisfies these requirements and is very easy to compute. The value of the weight function for grid cell (i,j) is calculated as:

$$w_{i,j} = \nabla^2(\phi)_{i,j} + w_{\min} \tag{1}$$

where ∇^2 is a discrete approximation to the Laplacian operator of the form

$$\nabla^2(\phi)_{i,j} = \frac{1}{4}\left(\phi_{i-1,j} + \phi_{i+1,j} + \phi_{i,j-1} + \phi_{i,j+1} - 4\phi_{i,j}\right) \tag{2}$$

which also represents the difference between the grid node value of field variable ϕ and the value obtained from the interpolation of ϕ values in the neighboring cells. A relatively small value of $\nabla^2\phi$ for any cell indicates that the grid can support relatively accurate interpolations of ϕ in the neighborhood of that cell. A minimum weight, $w_{\min}$, inhibits evacuation of grid nodes from regions of uniform ϕ.

The weight function above can result in the formation of concave or highly skewed grid cells. Since such grid cells are undesirable, a diffusive filter is applied to smooth this weight function (Srivastava et al., 2000). The final weight function is obtained by applying an area weighting to the smoothed weight function.

$$\tilde{w}_{i,j} = A_{i,j}^{1+e}\left(w_{i,j}^{\text{filtered}}\right) \tag{3}$$

The parameter e controls weighting with respect to the cell area A: a positive value gives more weight to larger cells and promotes gradual transitions from larger to smaller cells.

Repositioning of the grid nodes is accomplished by a *center-of-mass* scheme proposed by Eiseman (1987), which defines the new position of the grid node (k,l), $\vec{P}_{k,l}$, as:

$$\vec{P}_{k,l} = \frac{\sum_{i=k-1}^{k}\sum_{j=l-1}^{l} w_{i,j}\vec{Q}_{i,j}}{\sum_{i=k-1}^{k}\sum_{j=l-1}^{l} w_{i,j}} \tag{4}$$

where $\vec{Q}_{i,j}$ are the position vectors of the centroids of four cell sharing the grid node and $w_{i,j}$ are the values of the weight function at those locations.

If the maximum movement of all grid-nodes is below a preset tolerance, the grid is considered to have resolved the field sufficiently. Otherwise, the weight function is recomputed and the grid adaptation procedure is reiterated. The movement tolerance used here is, for any node, 5% of the distance to the closest node.

2.2. Emission source-grid cell intersection algorithm

Since the locations of the grid nodes have changed in the physical space, input data such as emissions must be re-gridded. As mentioned before, there are three major types of emissions being input into an AQM: emissions from point, line and area sources. Gridding of these emissions requires finding the intersections of each source type with the adapting grid cell. The structure of the grid at hand and the quadrilateral shape of the cells can be exploited to develop efficient intersection algorithms. This way the overhead involved in the re-gridding operations can be significantly reduced.

Intersecting point sources with the grid is the easiest one. A search is conducted over all grid cells to find out which one encloses the point source. The following algorithm has been developed. As illustrated in Fig. 1, starting from any vertex, two vectors are drawn: one to the next vertex in the counterclockwise direction and another to the point source location. If the cross product of the first vector with the second vector is negative (in a right-handed coordinate system), then the point source is outside this cell. In this case, checking the sign of the cross product is continued from the

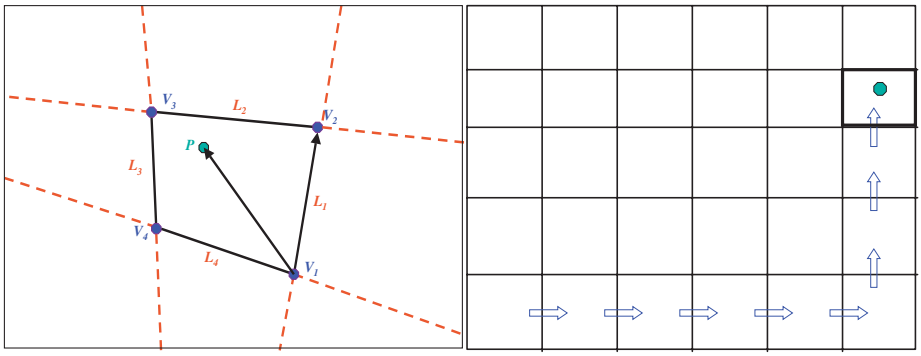

Fig. 1. Locating a point P in a grid cell (left). Arrows indicating the search as it proceeds to locate point P in N by M grid cells (right).

neighboring cell that shares with the original cell the side marked by the first vector above. In a structured grid where the cells are stored in an N by M array, finding this neighboring cell is trivial. If the cross product is positive, the process is continued from the next vertex of the cell. If the process yields positive cross products for all four vertices, then the point is inside that cell.

In general, the adaptive grid is initialized as a uniform grid. After the initial adaptation, the changes in pollutant fields during the air quality simulation are usually not dramatic enough to require a sudden adaptation from a uniform grid to a grid that can support a very complex field. In other words, the grid node movements would never be as large as they were in the initial adaptation step. In fact, it is very likely that the cell containing the point source prior to grid node repositioning would not move too far away from that source. Therefore, the point source can be located much faster by starting the search from the cell where it was found in the previous search.

Efficient algorithms that take advantage of the topology of the grid and small changes in pollutant fields have also been developed for line and area sources (Khan, 2003). Processing of line source emissions requires computing the length of each line source that falls within an adaptive grid cell. The line-polygon intersection process commences with identification of the grid cells that may fully or partially contain the source. Then, the point(s) of intersection of the line source with the grid cell sides are located. Unless the line source is wholly contained in a grid cell, the length of the line source that falls in a grid cell is either the distance between the line-source vertex in that grid cell and the intersection point or the distance between two intersection points. The amount of emission from the line source into the grid cell is calculated by taking the product of the line-source's length within that cell with its emission rate per unit length. For computational efficiency and as in case of point sources, the search for the grid cell(s) that contains the line-source vertices begins from the cell(s) where they were found the last time.

In case of area sources, which are specified on a uniform grid (referred to as the emissions grid), the fractional area of each emissions grid cell that intersects with the adaptive grid cell must be calculated. The intersection polygon is built by locating all

the intersection points of the adaptive and emission grid cell sides. For computational efficiency, the adaptive grid cell coordinates are used to select the emission grid cells that are likely to intersect the adaptive grid cell. The contribution of emissions from each overlapping polygon is summed up to provide the total area-source emissions emitted into the adaptive grid cell.

3. Applications to surface elevation data

The adaptive grid algorithm was applied to problems with increasing complexity and relevance to air quality modeling. Starting with pure advection tests (Srivastava et al., 2000), it was applied to reactive flows (Srivastava et al., 2001a) and to the simulation of a power-plant plume (Srivastava et al., 2001b). In all these applications, the adaptive grid solution was more accurate than a static, uniform grid solution obtained by using the same number of grid nodes. These applications, though being very relevant, had at best only a few flow features to be resolved. Here, the objective is to evaluate the potential performance of the algorithm in a regional-scale air quality simulation where hundreds of features such as puffs and plumes would have to be resolved simultaneously. To achieve this objective without performing an actual simulation, surface elevation data are used as a surrogate for pollutant concentration fields as described below.

The spatial distribution of surface elevation over complex terrain resembles pollutant concentration fields in many ways. Over large regions of flat surface such as oceans, lakes, valleys and plains, there are local features with large curvature in coastal areas, foothills, and mountain peaks. The only notable difference is that surface elevation is constant over time. However, recall that the grid adaptation procedure is applied by freezing the evolution of the pollutant field, thus, at any instant, the complexity of a pollutant field can be well represented by a surface elevation field. The application consists of reducing the number of data points by 75%. First, every other data point in x- and y-direction is eliminated. Then, the remaining points are relocated according to the curvature of the terrain. Finally, the ability of the grid-node relocation algorithm in retaining the accuracy of the original surface elevation data is evaluated.

Note that the purpose of this exercise is not to reproduce specific features of the terrain such as hill top lines. For surface elevation data, there are methods such as the very important point (VIP) method (Tsai, 1993) specifically designed for eliminating unimportant points from a uniform grid and retaining important ones. Triangulated irregular network (TIN) is the preferred method for storing large elevation data sets because of its efficiency and simple structure for accommodating irregularly spaced data points (e.g., Carter, 1988; Lee, 1989). Lee (1991) reviews and evaluates various methods for extracting TINs from dense digital elevation models (DEMs). TINs can accommodate finer resolution that is needed to define important small-scale features of the terrain. They may be stored in a hierarchical structure for applications that require different resolutions. (Scarlatos & Pavlidis, 1992). TINs typically require far less storage than regular grid DEMs to represent the same topography

(Goodrich, Woolhiser, & Keefer, 1991). TINs are not used in air quality modeling where the preferred data structure is the regular grid. It is much easier to solve the partial differential equations that define the time evolution of pollutant fields over regular or structured grids such as the adaptive grid used here.

Conversely, note that the adaptive grid algorithm has not been developed for the purpose of compressing regular grid DEM data. There are much better suited methods for that purpose. As the resolution of DEMs become finer, the level of data redundancy increases, especially if data points were sampled regularly. To minimize storage space, DEM data can be compressed by eliminating redundancy. For certain applications that can tolerate some constrained error, compromising data accuracy can further increase storage efficiency. A detailed review of data compression algorithms applied to regular grid DEMs can be found in Franklin (1995). Compression algorithms can be classified as lossless and "lossy" where "lossy" refers to the methods that introduce a controllable error to the original data. Some compression approaches use mathematical functions to approximate terrain, such as polynomials or quadtrees. Wavelets (Froment & Mallat, 1992) and fractals (Fisher, 1992) offer powerful alternatives for compressing surface elevation data. Kidner and Smith (1997, 2003) analyzed a number of different strategies for compressing DEM data. The search for better compression methods continues and is receiving significant attention from atmospheric researchers as the volume of available air pollution data increases rapidly.

3.1. Application to the United States–Mexico border area

The surface elevation data for the United States–Mexico border area (Joseph, 1997) were processed onto a uniform 136×80-cell fine grid with a 6.25-km resolution (Fig. 2). The same data were also mapped on a coarse grid with 68×40-grid cells, and uniform 12.5-km resolution. This second grid serves as the static grid with which

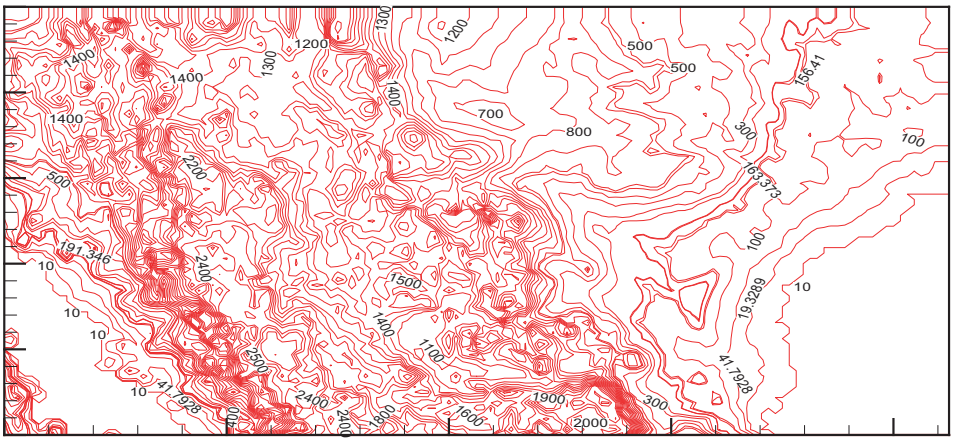

Fig. 2. Surface elevation for the United States–Mexico border area.

the adaptive grid is compared. It also constitutes the starting point for the adaptive grid. A weight function was computed based on the curvature of the terrain and the grid nodes were repositioned. After the coordinates of the adapted grid are computed in the physical space, the elevation of the grid nodes was obtained by bilinear interpolation from the fine grid. During this procedure, it is necessary to find the fine grid cell containing any given node of the adaptive grid. For this, we used the above described intersection algorithm developed to search for the grid cell that contains any given point source.

In order to assess if the adapted grid captures the surface elevation more accurately than the coarse grid, which is static and uniform, surface elevation from both grids is interpolated back onto the fine grid. Thus, there are three sets of surface elevation data on the fine grid: one from the DEM data set, another which is interpolated from the coarse grid, and a third one interpolated from the adaptive grid. These data sets are used in calculating and comparing the errors from the adaptive and coarse grids. The adaptation process is continued until all the node movements are below the preset relative tolerance of 5%.

The evolution of the grid during the adaptation process was visualized to see if the grid-repositioning algorithm created any highly skewed cells or voids in areas of flat terrain. The grid node movements were large in the beginning, but decreased as shown in Fig. 3. However, there were short periods during which large grid node movements were observed. These movements were almost always associated with the movement of boundary nodes that have only one degree of freedom. The grid movement tolerance was achieved after 353 iterations.

The final configuration of the grid is shown in Fig. 4. The transitions from coarse to fine resolution (or vice versa) are smooth and no highly skewed cells or voids are visible. In general, the grid nodes are clustered in regions with abrupt changes in surface elevation. Particularly noticeable is the clustering of grid nodes near the southern boundary where such changes are more prominent.

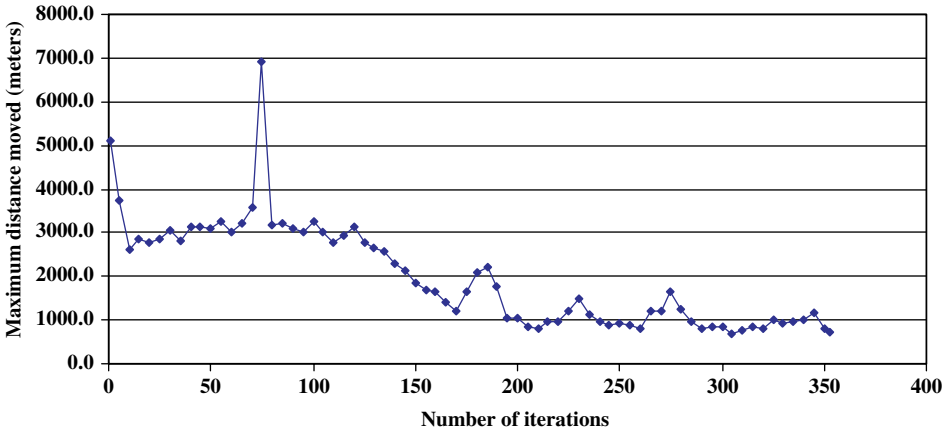

Fig. 3. Maximum distance moved by any grid node as a function of grid repositioning iterations in the application to the United States–Mexico border area.

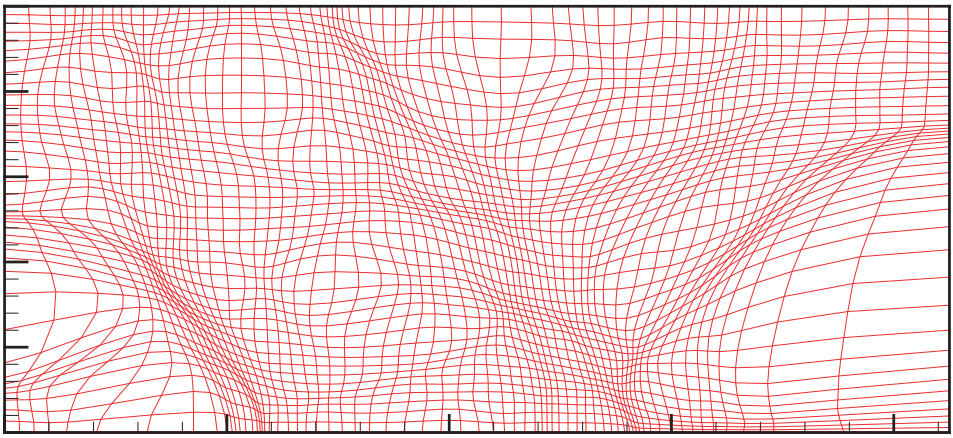

Fig. 4. The grid adapted to the terrain features of the United States–Mexico border area.

Note that there are uncertainties in the DEMs themselves but, for simplicity, it was assumed that DEM values are exact in the following error analysis. The difference between the interpolated surface elevation (either from the adaptive grid or from the coarse grid onto the fine grid) and the DEM data value at any fine grid node is defined as the nodal error:

$$E_{i,j} = \left| \phi_{i,j}^{\mathrm{DEM}} - \phi_{i,j}^{\mathrm{INTERPOLATED}} \right| \tag{5}$$

The domain wide maximum nodal error as a function of grid node repositioning iterations is shown in Fig. 5. Also shown in Fig. 5, is the maximum error for a sub-domain obtained by excluding all grid nodes that are located within 100 km of the domain boundary. The smaller maximum error for the sub-domain indicates that

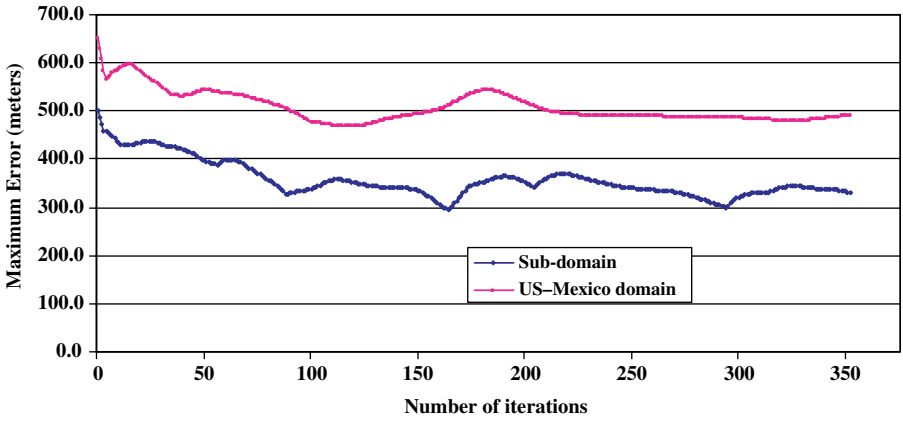

Fig. 5. Maximum error as a function of grid repositioning iterations in the application to the United States–Mexico border area.

the error is larger at nodes closer to the boundaries of the domain. This is due to the fact that boundary nodes are allowed to move in one-dimension only.

The maximum nodal error decreases from the initial value of 671 m, which is also the maximum error for the coarse grid, to 490 m after 353 iterations (Fig. 5). The increases in maximum error after periods of monotonic decrease correspond to shifts in maximum error from one area of the geographic domain to another. Recall that, since the number of nodes is fixed, the adaptive grid algorithm is clustering the nodes around one terrain feature at the expense of decreased resolution elsewhere. Therefore, while the local error around one terrain feature is decreased, it may start to increase around some other feature. The decreasing trend in the maximum error is promising and is much more pronounced in the sub-domain. In fact, the maximum error decreases substantially in the sub-domain, from 502 m to 329 m after 353 iterations. This suggests that the grid is converging towards a state where the domain-wide maximum error is minimized, although the final grid, which satisfied the node movement tolerance, does not correspond to the minimum local error.

In summary, the maximum error is 25% less on the adaptive grid than on a uniform coarse grid. The adaption and repositioning process is able to reduce the maximum error more efficiently at nodes that are located away from the boundaries of the domain. Maximum error in the sub-domain decreased by 35%. It was further observed, that the maximum error might shift from one location to another several times during the iterative grid-node repositioning process, and it is not necessarily minimized at the end, when the movement tolerance is met. The rate of convergence is not very fast, but since the grid-node repositioning algorithm is inexpensive (all 353 iterations were completed in 750 s on a 200 MHz processor) this does not pose a limitation. The resulting grid fulfills all of the requirements set forth for accurate numerical solution of partial differential equations.

3.2. Application to the Island of Hawaii

In the application above, the presence of prominent terrain features near the boundary had a significant impact on the results. The region surrounding the Island of Hawaii was selected for a second application. Since all the boundaries of this domain are over the ocean (Fig. 6(left)), the performance of the adaptive grid algorithm can be better assessed in this application. The surface elevation data from the DEM (USGS, 1997) were mapped onto a uniform 120×120-cell fine grid with a 4-km resolution. The same data were also processed on a coarse grid with 60×60-grid cells and uniform 8-km resolution. The procedure used in this application is the same as the one in the previous application.

There are no highly skewed cells present in the final configuration of the grid shown in Fig. 6(right). This configuration was achieved in 375 iterations. As desired, the grid nodes are clustered around the areas with sudden changes in surface elevation. The movement of the grid nodes decreased exponentially (Fig. 7) and in a more monotone fashion compared to the previous application (compare to Fig. 3). However, the rate at which the movement tolerance was achieved was approximately the same in both applications.

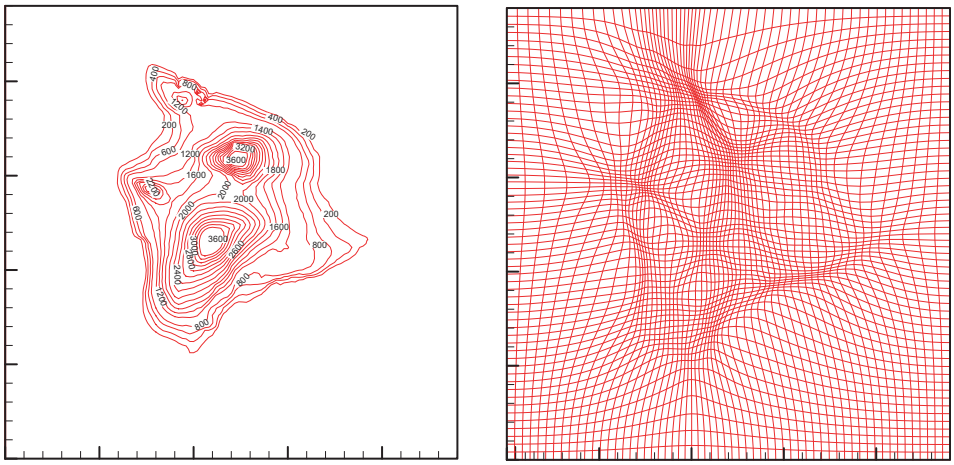

Fig. 6. Surface elevation for the Island of Hawaii (left) and the grid adapted to the terrain features (right).

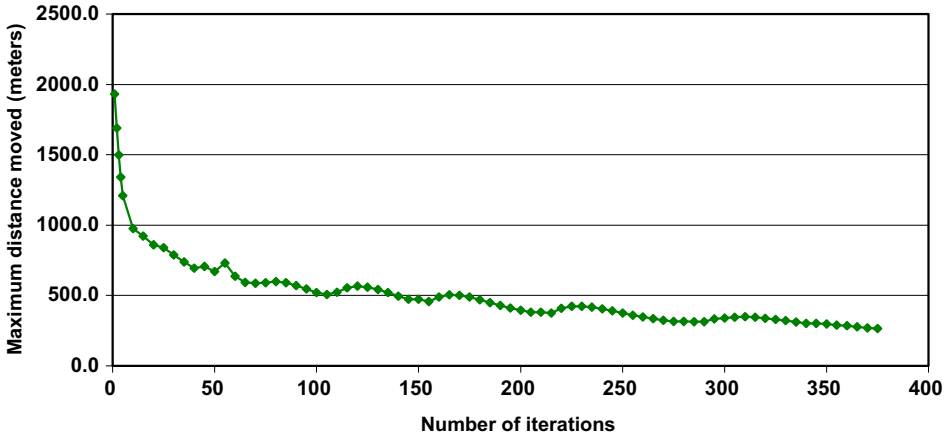

Fig. 7. Maximum distance moved by any grid node as a function of grid repositioning iterations in the application to the Island of Hawaii.

As shown in Fig. 8, the maximum nodal error, which had an initial value of 520 m, decreased by 60% to a value of 198 m after 375 iterations. During this general decrease, brief periods of increase are observed. These correspond to shifts in maximum error from one area of the geographic domain to another, as it was the case in the previous application. The decreasing trend in the global maximum error is more pronounced than in the previous application (compare to Fig. 5). Clearly, the grid is converging towards a state where the domain-wide maximum error is minimized, although the final grid, which satisfied the node movement tolerance, does not correspond to the minimum local error. In order to reduce the maximum error

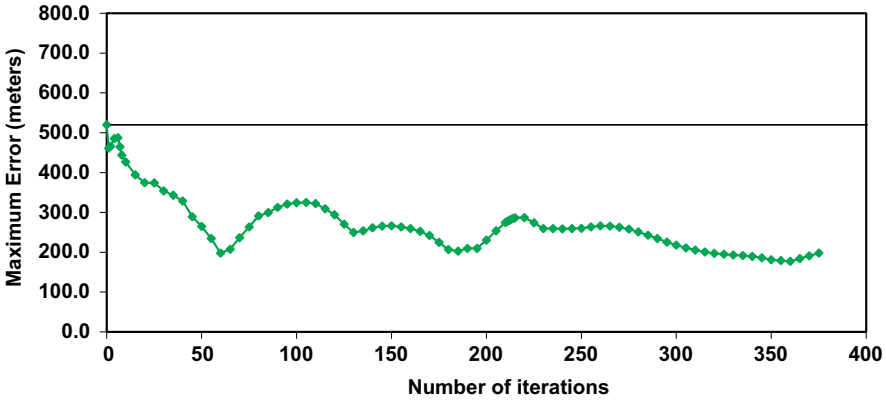

Fig. 8. Maximum error as a function of grid repositioning iterations in the application to the Island of Hawaii.

below 198 m, which is the minimum in Fig. 8, the number of grid nodes would have to be increased.

Also analyzed was the cumulative error defined as:

$$E^{\text{cum}} = \sum_{cg} \left|\phi^{\text{DEM}} - \phi^{\text{INTERPOLATED}}\right| + \sum_{fg} \left|\phi^{\text{DEM}} - \phi^{\text{INTERPOLATED}}\right| \tag{6}$$

As shown in Eq. (6), the cumulative error has two components. The first component is the error on the fine grid nodes that also belong to the coarse grid (*cg*) and the second component is the error at the remaining nodes of the fine grid (*fg*). After an initial period of increase (up to about the 10th iteration), there is an exponential decrease in cumulative error (Fig. 9). Clearly, the initial increase in the cumulative

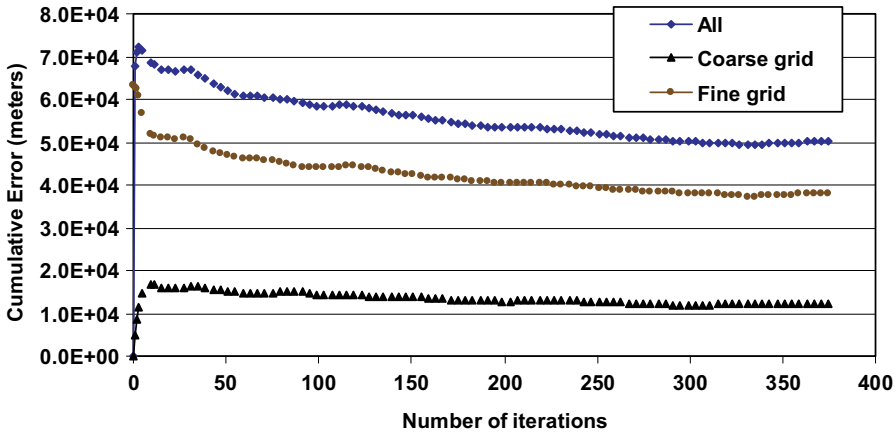

Fig. 9. Cumulative error and its breakdown to the nodes that are also on the coarse grid and those only present on the fine grid (for the application to the Island of Hawaii).

error is coming from the first component. Recall that the adaptive grid was initially the same as the coarse grid and that the surface elevation values for all the nodes were derived from the DEM data. Thus, the error at the nodes shared by the coarse and fine grids is zero. Once the node movement starts, the error at those nodes can only increase, but it reaches a plateau after about 15 iterations. Meanwhile, the cumulative error component for the nodes that are only on the fine grid decreases exponentially. At about the 10th iteration, the decrease in the second component offsets the increase in the first component, so the overall cumulative error starts decreasing. The monotonic decrease of the cumulative error afterwards shows that the grid adaptation is effectively increasing the accuracy of surface elevation, globally. Overall, the cumulative error decreased by more than 25% compared to the initial (coarse) grid.

In summary, the error in representing surface elevation data with four times fewer nodes than the original fine grid is smaller on the adaptive grid than the uniform coarse grid. Maximum error may shift from one location to another during the grid-node repositioning process. However, the cumulative error decreases almost monotonically indicating that the global error is effectively minimized.

4. Application to air quality data

The algorithms described above were incorporated in an AQM (Odman, Khan, & McRae, 2001). The model was applied to a historical air pollution episode over Tennessee Valley (Khan, 2003). Air quality simulations were conducted using a conventional static grid at 8-km resolution and an adaptive grid starting at a resolution of 8 km. Hence both grids use the same number of grid cells and they share the same vertical structure with 20 unequally spaced layers extending from the surface to 5340 m. Surface-layer nitrogen oxide (NO) concentration field was used in Eq. (1) to calculate the weight function that drives the grid adaptations. The adaptive grid simulation took about twice as long as the static grid. This is primarily due to the shorter time steps used in the adaptive grid simulation. Since the grid sizes are considerably smaller in regions of refinement, a much shorter time step is needed to keep the explicit transport schemes stable. A shorter time step means more frequent calls to process routines like diffusion and chemistry hence an increased computational overhead. The time spent in adapting the grid and intersecting the emissions with the grid cells is only a small fraction of the overall computational time.

NO is emitted from point, line and area sources as a combustion byproduct. It plays an important role in photochemical reactions leading to smog therefore AQMs should track the NO fields very accurately. Fig. 10 shows snapshots of the surface NO concentration fields from the static and adaptive grid simulations. Note that a number of isolated NO plumes from point sources are visible only in the adaptive grid simulation. The static grid simulation is unable to capture plumes from several industrial facilities and power plants in Tennessee, northern Alabama, central Georgia, and western South Carolina. Also of note is the ability of the adaptive grid to resolve steep concentration gradients near individual NO emission sources

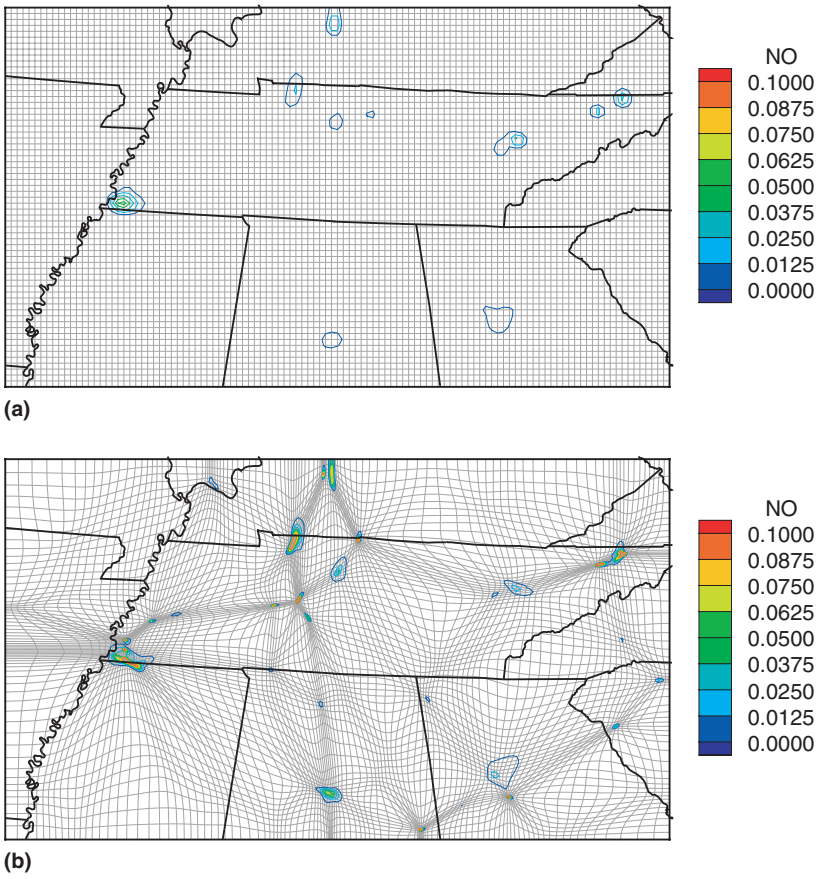

Fig. 10. Surface NO concentrations over Tennessee Valley on July 8th, 1995 at 1500 EST as predicted by the static (a) and adaptive (b) grid simulations.

throughout the domain as indicated by the increased number and closeness of the contours. The difference between the results of adaptive and static grid simulations clearly demonstrates the superior ability of the adaptive grid modeling technique to capture the details of pollutant plumes.

5. Conclusion

An adaptive grid AQM is being developed. In this paper, the grid node repositioning and the point-source–grid-cell intersection algorithms were evaluated, for both efficiency and accuracy, using surface elevation data. The algorithms were found efficient enough that the overhead of grid adaptations or re-gridding of emissions should not be restrictive in AQM simulations. The adaptive grid improves the accuracy considerably over a uniform grid with the same number of nodes. The

maximum error decreased by 25% due to grid adaptations in an application to the terrain of the United States–Mexico border area. The adaptive grid algorithm performs better when regions with large curvature in surface elevation are located away from the boundaries of the domain. This is evident from the analysis of error at nodes that are located more than 100 km from the domain boundaries. The decrease in maximum error at such nodes is 35%. In a second application to a region surrounding the Island of Hawaii where the changes in terrain slope are far away from the boundaries, the maximum error decreased by 60% and the cumulative error decreased by 25%. Finally, the algorithms described in this work were incorporated into the AQM. Application of the AQM to an air pollution episode in the Tennessee Valley indicates significant improvement in the ability to capture point source plumes at reasonable computational cost.

Acknowledgments

This work was supported by the US Environmental Protection Agency (Grant No. CR82505 and Assistance Agreement No. R 827028-01-0).

References

Alapaty, K., Mathur, R., & Odman, T. (1998). Intercomparison of spatial interpolation schemes for use in nested grid models. *Monthly Weather Review, 126*, 243–249.

Almgren, A. S., Bell, J. B., Collela, P., Howell, L. H., & Welcome, M. L. (1997). A high resolution adaptive projection method for regional atmospheric modeling. In Delic & Wheeler (Eds.), *Next generation environmental models and computational methods* (pp. 69). Philadelphia: Society For Industrial & Applied Mathematics.

Benson, R. A., & McRae, D. S. (1991). A solution adaptive mesh algorithm for dynamic/static refinement of two and three-dimensional grids. In *Proceedings of the third international conference on numerical grid generation in computational field simulations, Barcelona, Spain*.

Boylan, J. W., Odman, M. T., Wilkinson, J. G., Russell, A. G., Doty, K. G., Norris, W. B., & McNider, R. T. (2002). Development of a comprehensive multiscale "one atmosphere" modeling system: Application to the southern Appalachian mountains. *Atmospheric Environment, 36*, 3721–3734.

Carter, J. R. (1988). Digital representations of topographic surfaces. *Photogrammetric Engineering and Remote Sensing, 54*(11), 1577–1580.

Dietachmayer, G. S., & Droegemeier, K. K. (1992). Application of continuous dynamic grid adaption techniques to meteorological modeling. Part I: Basic formulation and accuracy. *Monthly Weather Review, 120*, 1675.

Eiseman, P. R. (1987). Adaptive grid generation. *Computational Methods and Application in Mechanical Engineering, 64*, 321.

Fisher, Y. (1992). A discussion of fractal image compression. In H.-O. Peitgen, H. Jürgens, & D. Saupe (Eds.), *Chaos and fractals* (pp. 903–919). New York: Springer-Verlag.

Franklin, W. R. (1995). Compressing elevation data. In *Advances in spatial databases, Proceedings of the fourth international symposium on large spatial databases (SSD'95), Portland, ME, August. Lecture Notes in Computer Science* (vol. 951, pp. 385–404). Berlin: Springer.

Froment, J., & Mallat, S. (1992). Second Generation Compact Image Coding with Wavelets. In C. K. Chui (Ed.). *Wavelets: A Tutorial in Theory and Applications* (vol. 2). NY: Academic Press.

Goodrich, D. C., Woolhiser, D. A., & Keefer, T. O. (1991). Kinematic routing using finite elements on a triangular irregular network. *Water Resources Research, 27*(6), 995–1003.

Joseph, D. (1997). Defense Mapping Agency 30 Seconds Elevations. Prepared and maintained by data support section, Scientific Computing Division, National Center for Atmospheric Research.

Karimi, H. A., Brandymeyer, J. E., Wong, D. C., & Bourgeois, A. J. (1999). A parallel polygon intersection algorithm for adaptive grid models. In *Proceedings of international conference on parallel and distributed processing techniques and application* (pp. 553–559).

Kessler, M. (1999). Development and analysis of an adaptive transport scheme. *Atmospheric Environment, 33*(15), 2347–2360.

Khan, M. N. (2003). Development and application of an adaptive grid air quality model. Ph.D. dissertation, School of Civil & Environmental Engineering, Georgia Institute of Technology, Atlanta, GA.

Kidner, D. B., & Smith, D. H. (1997). Storage-efficient techniques for representing digital terrain models. In Z. Kemp (Ed.). *Innovations in GIS* (vol. 4, pp. 25–41). London: Taylor & Francis.

Kidner, D. B., & Smith, D. H. (2003). Advances in the data compression of digital elevation models. *Computers & Geosciences, 29*, 985–1002.

Kumar, N., Odman, M. T., & Russell, A. G. (1994). Multiscale air quality modeling: Application to southern California. *Journal of Geophysical Research, 99*, 5385–5397.

Laflin, K. R., McRae, D. S. (1996). Three-dimensional viscous flow computations using near-optimal grid redistribution. In *Proceedings of first AFOSR conference on dynamic motion CFD*, Rutgers University, New Jersey.

Lee, J. (1989). A drop heuristic conversion method for extracting irregular network for digital elevation models. In *Proceedings of GIS/LIS '89 annual conference, Vol. 1* (pp. 30–39).

Lee, J. (1991). Comparison of existing methods for building triangular irregular network models of terrain from grid digital elevation models. *International Journal of Geographical Information Systems, 5*, 267–285.

Odman, M. T., Khan, M. N., & McRae, D. S. (2001). Adaptive grids in air pollution modeling: Towards an operational model. In S.-E. Gryning & F. A. Schiermeier (Eds.), *Air pollution modelling and its application XIV* (pp. 541–549). New York: Kluwer Academic/Plenum Publishers.

Odman, M. T., Mathur, R., Alapaty, K., Srivastava, R. K., McRae, D. S., & Yamartino, R. J. (1997). Nested and adaptive grids for multiscale air quality modeling. In G. Delic & M. F. Wheeler (Eds.), *Next generation environmental models and computational methods* (pp. 59–68). Philadelphia, PA: SIAM.

Odman, M. T., & Russell, A. G. (1991a). A multiscale finite element pollutant transport scheme for urban and regional modeling. *Atmospheric Environment, 25A*, 2385–2394.

Odman, M. T., & Russell, A. G. (1991b). Multiscale modeling of pollutant transport and chemistry. *Journal of Geophysical Research, 96*, 7363–7370.

Scarlatos, L., & Pavlidis, T. (1992). Hierarchical triangulation using cartographic coherence. *Graphical Models and Image Processing, 54*(2), 147–161.

Skamarock, W. C., & Kemp, J. B. (1993). Adaptive grid refinement for two-dimensional and three-dimensional non-hydrostatic atmospheric flow. *Monthly Weather Review, 121*, 788.

Srivastava, R. K., McRae, D. S., & Odman, M. T. (2000). An adaptive grid algorithm for air quality modeling. *Journal of Computational Physics, 165*, 437–472.

Srivastava, R. K., McRae, D. S., & Odman, M. T. (2001a). Simulation of a reacting pollutant puff using an adaptive grid algorithm. *Journal of Geophysical Research, 106*(24), 245–258.

Srivastava, R. K., McRae, D. S., & Odman, M. T. (2001b). Simulation of dispersion of a power plant plume using an adaptive grid algorithm. *Atmospheric Environment, 35*, 4801–4818.

Tomlin, A., Berzins, M., Ware, J., Smith, J., & Pilling, M. J. (1997). On the use of adaptive gridding methods for modelling chemical transport from multi-scale sources. *Atmospheric Environment, 31*, 2945–2959.

Tsai, V. J. D. (1993). Delaunay triangulations in TIN creation: An overview and a linear-time algorithm. *International Journal of Geographical Information Systems, 7*, 501–524.

USGS (1997). Digital Elevation Models for Hawaii. United States Geological Service. Available from http://edcwww.cr.usgs.gov/glis/hyper/guide/1_dgr_demfig/states/HI.html.